New Phytologist

Research

PKL is stabilized by MMS21 to negatively regulate *Arabidopsis* drought tolerance through directly repressing *AFL1* transcription

Yexing Jing[1], Ziyi Yang[1], Ruizhen Yang[1], Yunwei Zhang[1], Weihua Qiao[1], Yun Zhou[2] and Jiaqiang Sun[1]

[1]State Key Laboratory of Crop Gene Resources and Breeding, Institute of Crop Sciences, Chinese Academy of Agricultural Sciences, Beijing 100081, China; [2]State Key Laboratory of Crop Stress Adaptation and Improvement, School of Life Sciences, Henan University, Kaifeng 475001, China

Author for correspondence:
Jiaqiang Sun
Email: sunjiaqiang@caas.cn

Received: *3 January 2023*
Accepted: *20 April 2023*

New Phytologist (2023)
doi: 10.1111/nph.18972

Key words: *AFL1*, *Arabidopsis*, drought tolerance, MMS21, PKL, protein stability.

Summary

- Drought stress causes substantial losses in crop production per year worldwide, threatening global food security. Identification of the genetic components underlying drought tolerance in plants is of great importance. In this study, we report that loss-of-function of the chromatin-remodeling factor PICKLE (PKL), which is involved in repression of transcription, enhances drought tolerance of *Arabidopsis*.
- At first, we find that PKL interacts with ABI5 to regulate seed germination, but PKL regulates drought tolerance independently of ABI5. Then, we find that PKL is necessary for repressing the drought-tolerant gene *AFL1*, which is responsible for the drought-tolerant phenotype of *pkl* mutant. Genetic complementation tests demonstrate that the Chromo domain and ATPase domain but not the PHD domain are required for the function of PKL in regulating drought tolerance. Interestingly, we find that the DNA-binding domain (DBD) is essential for the protein stability of PKL.
- Furthermore, we demonstrate that the SUMO E3 ligase MMS21 interacts with and enhances the protein stability of PKL. Genetic interaction analysis shows that MMS21 and PKL additively regulate plant drought tolerance.
- Collectively, our findings uncover a MMS21-PKL-*AFL1* module in regulating plant drought tolerance and offer insights into a novel strategy to improve crop drought tolerance.

Introduction

Drought is a major abiotic stress that dramatically limits plant growth and crop productivity (Zhu, 2002; Hu & Xiong, 2014; Lesk *et al.*, 2016). Therefore, understanding how plants adapt to adverse environmental conditions is critical for global food security. However, the identification of the genetic components underlying drought tolerance has proven to be challenging.

To cope with the drought stress, plants have evolved a complex regulatory mechanism to adapt to this adverse environmental condition (Gupta *et al.*, 2020). Under drought stress, the concentration of abscisic acid (ABA) can significantly increase, and activates downstream signaling pathway (Zeevaart, 1980; Okamoto *et al.*, 2013; Park *et al.*, 2015; Kalladan *et al.*, 2017; Kuromori *et al.*, 2018; Wang *et al.*, 2018; Mega *et al.*, 2019; Vaidya *et al.*, 2019), which has key roles in enhancing drought tolerance in several species. A recent study reveals that the sucrose transporters SWEET11 and SWEET12 are phosphorylated by ABA-activated SnRK2s and transport sucrose from shoots to roots in *Arabidopsis*, providing a strategy for plant adaptation to drought stress (Chen *et al.*, 2022). In rice and wheat, overexpression of the ABA receptors *PYLs* confers ABA hypersensitivity and drought tolerance (Kim *et al.*, 2012, 2014; Tian *et al.*, 2015; Dittrich *et al.*, 2019; Santosh Kumar *et al.*, 2021; Mao *et al.*, 2022). Overexpression of the membrane-associated protein At14a-like1 (AFL1) led to increased drought tolerance in *Arabidopsis* (Kumar *et al.*, 2015).

In *Arabidopsis*, trimethylation of histone H3 Lys 27 (H3K27me3) is deposited by Polycomb Repressive Complex 2 (PRC2; Hinsch *et al.*, 2021). PICKLE (PKL) is an ATP-dependent Chromodomain Helicase DNA-binding domain type 3 (CHD3) chromatin remodeler that is required for H3K27me3 deposition at some genomic locations and regulates multiple plant developmental and physiological processes (Tong *et al.*, 1998; Ogas *et al.*, 1999; Fukaki *et al.*, 2006; Perruc *et al.*, 2007; Aichinger *et al.*, 2009, 2011; Furuta *et al.*, 2011; Jing *et al.*, 2013, 2019a,b; Zhang *et al.*, 2014; Xu *et al.*, 2016; Zha *et al.*, 2017, 2020; Yang *et al.*, 2019; Hinsch *et al.*, 2021; Hu *et al.*, 2022; Liang *et al.*, 2022). A recent study revealed that PKL could interact with the transcription factors VIVIPAROUS1/ABI3-LIKE1/2 (VAL1/2) to repress the expression of *ABA INSENSITIVE 3* (*ABI3*) and *AGAMOUS-LIKE 15* (*AGL15*) in regulating the seed-to-seedling transition (Liang *et al.*, 2022). However, whether and how PKL plays a role in regulating plant drought tolerance remain obscure.

Ubiquitination and SUMOylation are two kinds of post-translational modification (Han *et al.*, 2021). The ubiquitinated proteins are usually distinguished and recognized by the 26S proteasome for degradation (Sadanandom *et al.*, 2012). SUMOylation is a kind of reversible post-translational modification conjugating activated SUMO peptides to target proteins. In *Arabidopsis*, the core SUMOylation enzymes include E1 activation enzymes (SAE1a, SAE1b, and SAE2), an E2 conjugation enzyme (SCE1), and E3 ligases (MMS21 and SIZ1; Kurepa *et al.*, 2003; Miura *et al.*, 2007; Gareau & Lima, 2010; Miller *et al.*, 2010). The SUMOligase MMS21 plays essential roles in plant development and stress response (Huang *et al.*, 2009; Ishida *et al.*, 2009; Xu & Yang, 2013; Zhang *et al.*, 2013; Liu *et al.*, 2014; Yuan *et al.*, 2014; Liu *et al.*, 2016; Zhang *et al.*, 2017).

In this study, we find that the loss-of-function mutant of PKL displays a drought-tolerant phenotype. Our results reveal that PKL represses the expression of the drought-tolerant gene *AFL1* via facilitating the H3K27me3 deposition at the chromatin regions *AFL1*. Genetic evidence suggests that the regulatory role of PKL in plant drought tolerance is dependent on *AFL1*. Furthermore, we find that MMS21 directly interacts with and stabilizes PKL to additively regulate drought tolerance. Collectively, our work reveals a MMS21-PKL-*AFL1* module in regulating *Arabidopsis* drought tolerance.

Materials and Methods

Plant materials and growth conditions

All plants used in this study are in the Columbia (Col-0) ecotype background. The *pkl* mutant (GK_273E06) was obtained from the Arabidopsis Biological Resources Center (ABRC). Some of the transgenic lines and the mutant plants used in this study were previously described: *PKLp:PKL-GFP* (Aichinger *et al.*, 2011), *35S:Myc-MMS21* (Yu *et al.*, 2019), *mms21-1* (Zhang *et al.*, 2013), and *abi5-7* (Nambara *et al.*, 2002). To generate the *35S:ABI5-Flag* transgenic plants, the CDS sequence of *ABI5* gene was amplified and inserted into the *p1300-35S-Flag* vector. The full-length coding region or truncated coding region of *PKL* was amplified and cloned into the *PKLp:GFP* construct containing the *PKL* promoter (2000 bp) to generate the *PKLp:PKL-GFP*; *PKLp:PKLΔPHD-GFP*; *PKLp:PKLΔChromo-GFP*; *PKLp:PKLΔATPase-GFP*; and *PKLp:PKLΔDBD-GFP* constructs. These constructs were introduced into the *A. tumefaciens* strain GV3101 and then transformed into the *pkl* mutant plants via the floral dip method to generate corresponding transgenic plants (Clough & Bent, 1998). The *afl1* mutant was obtained using a CRICPR/Cas9 system (Yan *et al.*, 2015). A 20-nt target of *AFL1* was cloned into pCAMBIA1300-*pYAO*:Cas9 vector and then transformed into Col-0 by floral dip method (Clough & Bent, 1998). The double mutants *pkl abi5-7*, *pkl afl1*, and *mms21-1 pkl* were generated by genetic crossing. All the *Arabidopsis thaliana* seeds were placed at 4°C for 2 d and moved to the growth conditions under LD (16 h : 8 h, light : dark) at 22°C. *N. benthamiana* was grown in a glasshouse at 25°C with a 16 h : 8 h, light : dark cycle.

Phenotypic analyses

For the drought tolerance assay, 7-d-old seedlings were transferred into soil and grown for another 21 d. The 4-wk-old plants were subjected to progressive drought for 7–10 d, and survival rates were then determined after rewatering for 2 d. For the water loss assay, the rosette leaves of 4-wk-old plants were detached, and then placed on a piece of weighing paper. The weight at the indicated time was measured (1, 2, 3, and 4 h). Water loss is shown as a percentage of the original fresh weight.

The ABA/mannitol-induced stomatal closure assays were carried out as described previously (Chen *et al.*, 2021). The 10-d-old seedlings were floated in MES buffer (10 mM 2-[N-morpholino] ethanesulfonic acid (MES)-KOH, pH 6.15, 10 mM KCl, and 50 μM $CaCl_2$) for 2 h under the light at 22°C, to induce stomatal opening. And then seedlings were transferred to MES buffer containing 10 μM ABA or 300 mM mannitol for 2–3 h or 4 h, respectively. Stomatal apertures were recorded under confocal microscopy (LSM880; Carl Zeiss). Stomatal aperture was measured using ImageJ software.

The greening assay was carried out as described in the previous study with minor modifications (Ju *et al.*, 2019). Seeds of Col-0 and the mutants were disinfected and sown on half-strength Murashige & Skoog medium (½ MS) supplemented with 0.5 μM ABA under LD (16 h : 8 h, light : dark) conditions at 22°C. Cotyledon greening is defined as an obvious observation of green cotyledons in a seedling. Three independent experiments were performed and similar results were obtained.

RNA extraction and real-time PCR

Total RNA was extracted using Trizol reagent (Invitrogen) according to the manufacturer's instructions. cDNA was prepared from 2 μg of total RNA and 5× All-In-One RT MasterMix system (Applied Biological Materials, Richmond, Canada), following the manufacturer's instructions. Reverse transcriptase–polymerase chain reaction (RT-qPCR) was performed using SYBR Premix Ex Taq (TaKaRa, Kusatsu, Japan) on a LightCycler 96 instrument (Roche). Expression levels of target genes were normalized to *ACTIN7* using the $2^{-\Delta\Delta C_t}$ method. Each experiment was performed independently three times. Primers are listed in Supporting Information Table S1.

Protein extraction and immunoblotting

Seedlings were treated with different chemicals. For protein level analyses, total proteins were extracted using protein extraction buffer (125 mM Tris–HCl at pH 6.8, 4% SDS, 20% glycerol, 0.001% bromophenol blue) with freshly added 2% b-mercaptoethanol. The following antibodies were used: anti-GFP (1 : 2000; 11814460001; Roche), anti-Flag (1 : 5000; M185-3l; MBL, Nagoya, Japan), anti-PKL (1 : 5000), anti-Myc (1 : 5000; 11667149001; Roche), anti-SUMO1 (Ab5316; Abcam, Cambridge, UK), anti-mouse IgG (1 : 75000; A9044-2ML; Sigma), and anti-rabbit IgG (1 : 3000; Sigma) antibodies. Actin (1 : 5000; CW0264M; CWBIO, Beijing, China) was used an internal control.

LCI assays

The LCI assays for the protein interaction detection were performed in *N. benthamiana* leaves as described previously (He *et al.*, 2019). The full-length coding regions or truncated derivatives was amplified and cloned into the pCAMBIA1300-nLUC and pCAMBIA1300-cLUC vectors with 35S promoter (Chen *et al.*, 2008). Primers are listed in Table S1. *A. tumefaciens* strain GV3101 bacteria carrying different constructs were co-infiltrated into *N. benthamiana* leaves. LUC activities were analyzed after 48 h infiltration using NightSHADE LB 985 (Berthold, Bad Wildbad, Germany). Three biological replications were performed with similar results.

BiFC assays

The coding sequences of *PKL*, *ABI5*, and *MMS21* were fused with N-terminal YFP with 35S promoter (nYFP-ABI5 and nYFP-MMS21) and C-terminal YFP with 35S promoter (cYFP-PKL) using Gateway system (Ju *et al.*, 2019). *A. tumefaciens* strain GV3101 was transformed with the constructs and then infiltrated into. *N. benthamiana* leaves. After 48 h infiltration, fluorescence signals of yellow fluorescent protein (YFP) were observed with confocal microscopy (LSM880; Carl Zeiss). Images were captured at 514 nm laser excitation and 519–620 nm emission for YFP.

Generation of polyclonal anti-PKL antibody

The anti-PKL polyclonal antibody was raised by ABclonal Biotechnology Co. Ltd (ABclonal), Beijing, China. The specific polypeptide 5′-MSSLVERLRIRSDRKPVYNLDDSDDDDFVP KKDRTFEQVEAIVRTDAKENACQACGESTNLVSCNTCT YAFHAKCLVPPLKDASVENWRCPECVSPLNEIDKILDCE-3′ was synthesized and used as antigen for immunization of rabbits for polyclonal antiserum production. Antigen-affinity purified antibody was used in immunoblotting.

Co-immunoprecipitation assays

Col-0 and the transgenic plant *35S:ABI5-Flag* were used for the interaction analysis between PKL and ABI5 *in vivo*. Col-0 and the transgenic plant *35S:Myc-MMS21* were used for the interaction analysis between PKL and MMS21 *in vivo*. The 7-d-old seedlings were collected, and total proteins were extracted using lysis buffer (50 mM Tris–HCl at pH 7.5, 150 mM NaCl, 5 mM EDTA at pH 8.0, 0.1% Triton X-100, 0.2% NP-40, freshly added 1 mM PMSF, Complete Protease Inhibitor cocktail (Roche), and 10 μM MG132). The extracts were centrifuged at 4°C for 20 min. 20 μl Dynabeads protein G Beads (Invitrogen catalog number 10003) were incubated with the supernatant to reduce nonspecific immunoglobulin binding for 1 h, and subsequently incubated with 30 μl anti-Myc/anti-FLAG (MBL, M047-10; MBL, M185-10) conjugated beads at 4°C overnight. The beads were washed five times with lysis buffer. The immunoprecipitates were then separated on SDS-polyacrylamide gels and detected by immunoblotting with anti-PKL, anti-Flag, and anti-Myc antibodies.

RNA-sequencing and data analysis

The 6-d-old seedlings of the *pkl* mutant and Col-0 with or without ABA treatment were collected and total RNA was extracted using TRIzol reagent (Invitrogen). Three replicates were employed for each sample. cDNA libraries were generated and further sequenced on Illumina HiSeq. 2000 platform (Illumina Inc., San Diego, CA, USA). After screening and trimming, clean reads were mapped to the reference genome of *Arabidopsis thaliana* (TAIR10, www.arabidopsis.org) using the TopHat2 software. Cufflinks methods were used for determination of expression values. Genes with estimated absolute fold changes ≥ 2 were identified as reliable differentially expressed genes (DEGs).

Chromatin immunoprecipitation assays

Chromatin immunoprecipitation (ChIP) experiments were performed as described previously (Yang *et al.*, 2021). The 10-d-old seedlings of Col-0, *PKLp:PKL-GFP/pkl* and the *pkl* mutant were used for the ChIP assays. About 2 g of each sample was harvested and crosslinked in 1% formaldehyde for 15 min, then stopped by neutralization with 0.25 M glycine. After washing for five times with distilled water, the seedlings were grounded to powder in liquid nitrogen. Total chromatin was extracted, sheared by sonication and immunoprecipitated using anti-GFP antibody (Abcam ChIP grade, ab290) or anti-H3K27me3 antibody (07-449; Millipore, Darmstadt, Germany). The precipitated DNA was eluted and the enrichment of DNA fragments was analyzed by real-time qPCR with specific primers, as shown in Table S1. The enrichments were relative to INPUT.

Analysis of phylogeny, gene structure, and conserved domains

The full-length amino acid sequences were aligned using ClustalW for the phylogenetic tree construction. The phylogenetic trees were constructed using the neighbor-joining method on Mega-X with a number of Bootstrap replications as 500 (Kumar *et al.*, 2018). We chose the p-distance method for the quantification of phylogenetic trees. Gene Structure Display Server (GSDS) v.2.0 was used for visualization of the gene structures (Guo *et al.*, 2007). Domain analysis was carried out using the web tool InterProScan (http://www.ebi.ac.uk/interpro/).

Accession numbers

Sequence data in *Arabidopsis* in this study can be found in the *Arabidopsis* Genome Initiative database under the following accession numbers: *PKL* (At2g25170), *AFL1* (At3g28270), *MMS21* (At3g15150), *ABI3* (At3g24650), *ABI4* (At2g40220), *ABI5* (At2g36270), *SUMO1* (At4g26840), *SUMO3* (At5g55170), *HAI2* (At1g07430), *COR15A* (At2g42450), and *ACTIN7* (At5g09810).

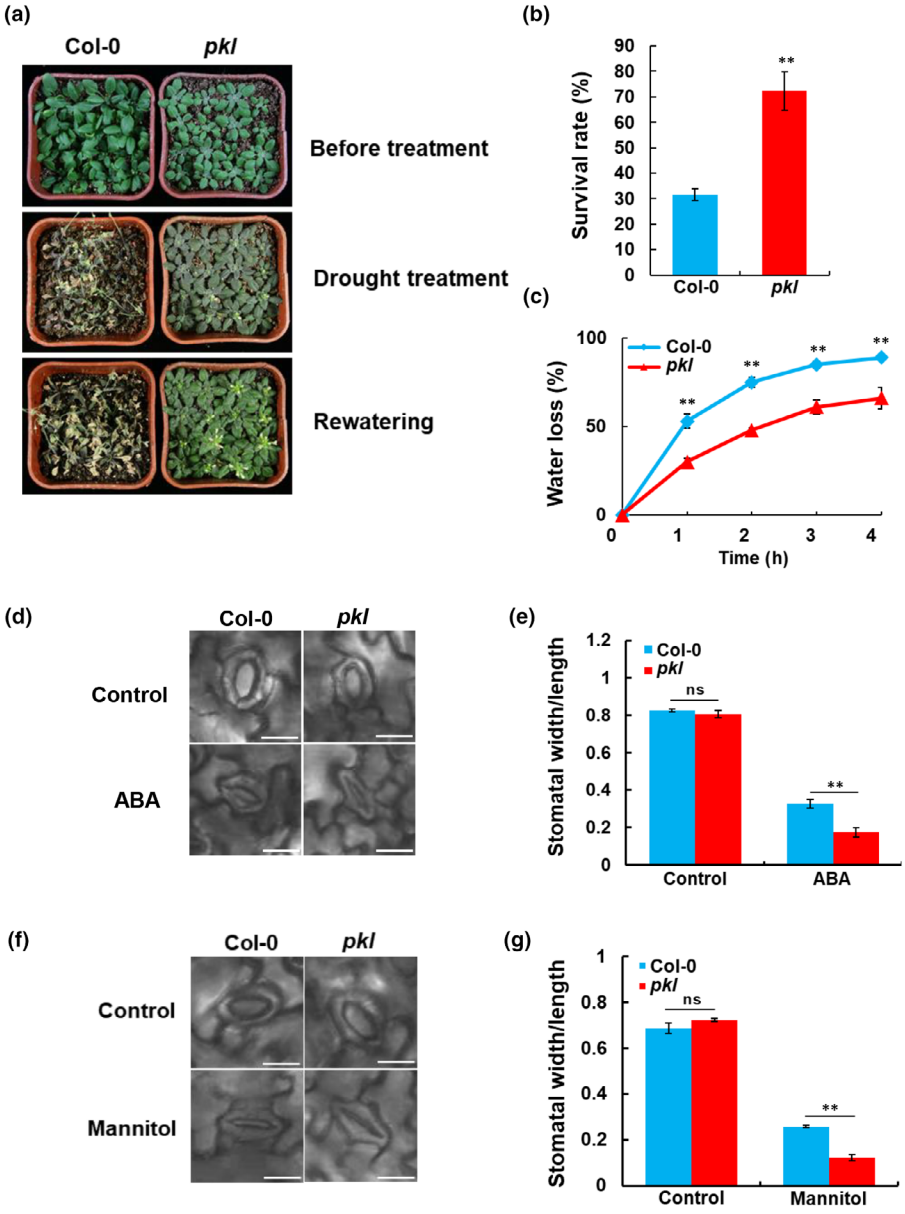

Fig. 1 PICKLE (PKL) negatively regulates plant drought tolerance in *Arabidopsis*. (a, b) Drought-tolerant phenotypes (a) and survival rates (b) of soil-grown *pkl* mutant. Four-week-old plants were dehydrated for 7–10 d and then rehydrated for 2 d. Values in (b) represent means ± SD obtained from three replicates with 48 plants per replicate. Statistical significance was determined by Student's *t*-test: **, $P < 0.01$. (c) Water loss rates of leaves detached from Col-0 and the *pkl* mutant. Means and SD of water loss rates were obtained from three replicates. Statistical significance was determined by Student's *t*-test: **, $P < 0.01$. (d) Stomatal aperture of Col-0 and the *pkl* mutant in the presence of 10 μM abscisic acid (ABA) treatment. Bars, 20 μm. (e) Statistical analysis of stomatal aperture (the ratio of width to length) shown in (d). Values are means ± SD ($n = 30$). Statistical significance was determined by Student's *t*-test: **, $P < 0.01$; ns, not significant. (f) Stomatal aperture of Col-0 and the *pkl* mutant in the presence of 300 mM mannitol treatment. Bars, 20 μm. (g) Statistical analysis of stomatal aperture (the ratio of width to length) shown in (f). Values are means ± SD ($n = 30$). Statistical significance was determined by Student's *t*-test: **, $P < 0.01$; ns, not significant.

Results

Loss of PKL confers a drought-tolerant phenotype

To explore whether PKL play a role in regulating drought tolerance, we evaluated the drought stress response of the *pkl* mutant. We stopped irrigation of 4-wk-old Col-0 and the *pkl* mutant for 7–10 d and then rewatered them. Plant survival rates were scored 2 d after rewatering. We observed higher survival rate of the *pkl* mutant (*c.* 72% on average) than that of Col-0 (*c.* 32% on average; Fig. 1a,b). Furthermore, we performed water loss analysis in detached leaves and found that the rate of water loss in the *pkl* mutant was slower than that in Col-0 (Fig. 1c). To verify the correlation between rates of water loss and stomatal aperture, we analyzed stomatal aperture of Col-0 and the *pkl* mutant. The result showed that stomatal aperture in the leaves of *pkl* mutant are smaller than that in Col-0 in the presence of 10 μM ABA treatment (Fig. 1d,e). We also analyzed stomatal aperture of Col-0 and the *pkl* mutant in response to mannitol treatment (mimic drought stress). The result showed that stomatal aperture in the leaves of *pkl* mutant are also smaller than that in Col-0 in the presence of 300 mM mannitol treatment (Fig. 1f,g). These results reveal that PKL negatively regulates drought tolerance probably through influencing stomatal aperture in *Arabidopsis*.

It is well known that ABA plays an important role in regulating abiotic stress responses, especially for salt and drought stresses (Zhu, 2002; Miao *et al.*, 2020; Lim *et al.*, 2022). We sought to investigate the relationship between PKL and ABA signaling in the regulation of plant drought tolerance. To test this idea, we evaluated physical interactions between PKL and some transcriptional factors (TFs) in ABA signaling by firefly luciferase (LUC) complementation imaging (LCI) assays. The ABA signaling TFs

ABI3, ABI4, and ABI5 were separately fused to the C-terminal part of LUC to generate the cLUC-ABI3, cLUC-ABI4, and cLUC-ABI5 constructs, and PKL was fused to the N-terminal part of LUC to generate the nLUC-PKL construct. Only when cLUC-ABI5 and nLUC-PKL were co-expressed in *N. benthamiana* leaves, strong LUC activity could be detected (Fig. S1a), suggesting that PKL could interact with ABI5 but not with ABI3 or ABI4. Furthermore, we confirmed that PKL physically interacts with ABI5 using bimolecular fluorescence complementation (BiFC) assays. ABI5 was fused to the N-terminal part of YFP (nYFP-ABI5) and PKL was fused to the C-terminal part of YFP (cYFP-PKL). The result showed that the interaction of PKL and ABI5 occurs in the nucleus (Fig. S1b). We next employed co-immunoprecipitation (Co-IP) assays to further validate the interaction between PKL and ABI5 *in vivo* by extracting proteins from Col-0 and *35S:ABI5-Flag* transgenic plants. To this end, we generated a specific antibody raised against recombinant PKL. The PKL antibody recognized a specific band of the expected molecular weight for PKL in Col-0 protein extract, but not in the *pkl* mutant extract (Fig. S1c). Co-immunoprecipitation assays demonstrated that PKL could be immunoprecipitated by ABI5-Flag (Fig. S1d), indicating that PKL indeed interacts with ABI5 in *Arabidopsis*. To determine whether ABI5 is involved in PKL-mediated regulation of drought tolerance, we generated the double mutant *pkl abi5* via genetic crossing between the *pkl* and *abi5-7* mutants. Then we evaluated the drought stress responses of Col-0, *pkl*, *abi5-7*, and *pkl abi5-7*. The results showed that the *abi5-7* mutant and Col-0 exhibited similar drought stress responses, while the *pkl abi5-7* double mutant exhibited a drought-tolerant phenotype similar to the *pkl* mutant (Fig. S2), indicated that the drought-tolerant phenotype of the *pkl* mutant is independent of ABI5. To further explore the relationship between PKL and ABI5, we evaluated the cotyledon greening rates of Col-0, *pkl*, *abi5-7* and *pkl abi5-7* on ½MS medium supplemented with 0.5 μM ABA. The results showed that the *pkl* mutant had lower cotyledon greening rate than Col-0, while *abi5-7* and *pkl abi5-7* had higher cotyledon greening rates than Col-0 in the presence of ABA application (Fig. S3). These results demonstrated that PKL regulates the ABA-mediated inhibition of seedling growth dependently on ABI5. Taken together, PKL interacts with ABI5 to regulate seedling growth in an ABI5-dependent manner, while PKL regulates drought tolerance independently of ABI5.

Functional analyses for the different domains of PKL in regulating drought tolerance

PKL harbors four different domains including chromatin organization modifier domain (Chromo domain), SWI2/SNF2 ATPase/Helicase domain (ATPase domain), DNA-binding domain (DBD domain), and PHD zinc finger domain (PHD domain; Ho *et al.*, 2013; Fig. S4a). To investigate the roles of different PKL domain in regulating plant response to drought stress, we generated a series of transgenic lines with the native *PKL* promoter and full-length coding sequence (CDS) or truncated CDS in the *pkl* mutant background: *PKLp:PKL-GFP/pkl* (PKL); *PKLp:PKLΔPHD-GFP/pkl* (ΔPHD); *PKLp:PKLΔChromo-GFP/pkl* (ΔChromo); *PKLp:PKLΔATPase-GFP/pkl* (ΔATPase); and *PKLp:PKLΔDBD-GFP/pkl* (ΔDBD). Then we examined the drought stress response of these transgenic lines. The drought stress responses of PKL and ΔPHD transgenic plants were similar to that of Col-0, indicating that PKL and PKLΔPHD could rescue the drought-tolerant phenotype of *pkl* mutant, respectively. However, the PKLΔChromo, PKLΔATPase, and PKLΔDBD failed to rescue the drought-tolerant phenotype of *pkl* mutant (Fig. 2a). Survival rates of these plants were correlated with their drought stress responses. After drought and rewatering, 75% of the *pkl* mutant plants survived, similar with ΔChromo (*c.* 68% on average), ΔATPase (*c.* 69% on average), and ΔDBD (*c.* 72% on average); whereas only 30% of Col-0 survived, similar with PKL (*c.* 32% on average) and ΔPHD (*c.* 30% on average; Fig. 2b). Water loss analysis in detached leaves showed that water loss rates of the detached leaves of these PKL and ΔPHD transgenic plants were largely similar to that of Col-0, whereas the ΔChromo, ΔATPase, and ΔDBD transgenic plants were similar to the *pkl* mutant (Fig. 2c). These results demonstrated that the Chromo domain, ATPase domain and DBD domain but not the PHD domain are necessary for PKL to regulate plant drought stress response.

Because PKL is not only involved in drought stress response, but also in plant growth and development, we evaluated whether these truncated versions of PKL can complement the function of PKL in plant growth and development. We observed the plant developmental phenotypes of the *pkl* mutant and these transgenic plants in the *pkl* mutant background. The results showed that the plant height of the *pkl* mutant was obviously lower than Col-0. While plant height of the full-length PKL transgenic plants was largely similar to that of Col-0, indicating that the full-length PKL could rescue the plant growth defect of *pkl* mutant. However, the PKLΔPHD, PKLΔChromo, PKLΔATPase, and PKLΔDBD could partially rescue or failed to rescue the plant growth defect of *pkl* mutant (Fig. S4b,c). These results demonstrated that the Chromo domain, ATPase domain, DBD domain as well as the PHD domain are required for PKL to promote plant growth.

The DBD domain is required for the stability of PKL

We further analyzed the transcript and protein levels of full-length or truncated PKL in transgenic plants. RT-qPCR analysis showed that the transcript levels of *PKL* were largely similar, except for the higher transcript level in the ΔATPase transgenic plants (Fig. 2d). Then we detected the protein levels of PKL in these transgenic plants. The result showed that the protein levels of PKL were similar in the PKL, ΔPHD, ΔChromo, and ΔATPase transgenic plants (Fig. 2e). Notably, we found that the protein level of PKL in the ΔDBD transgenic plants was undetectable, whereas MG132, a specific inhibitor of the 26S proteasome, could rescue its protein level (Fig. 2f). Simultaneously, MG132 treatment could increase the protein level of PKL in the PKL transgenic plants (Fig. 2f). To exclude the effect of expression levels on the protein levels of PKL, we tested the expression

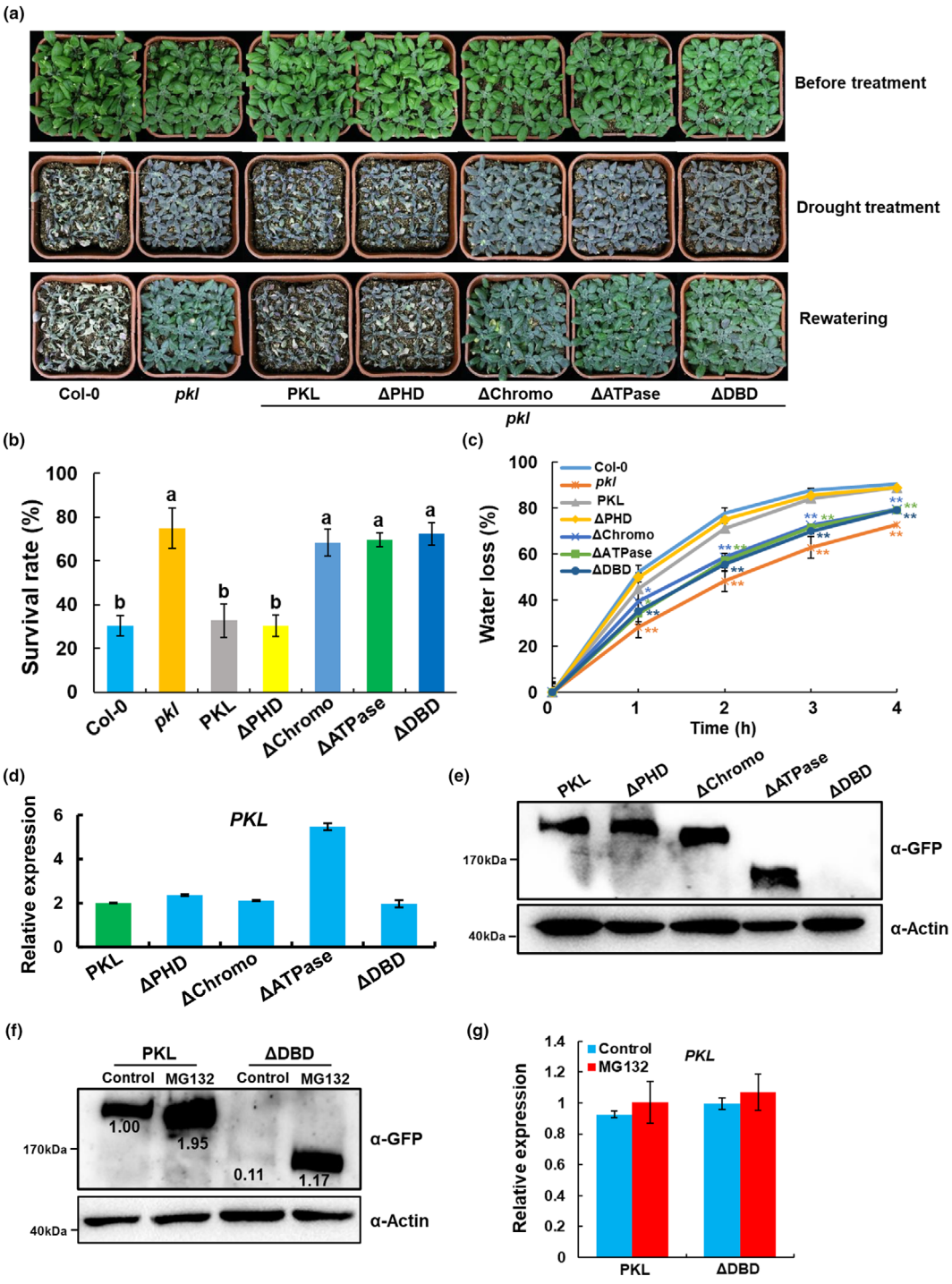

Fig. 2 Genetic complementation verifies the roles of different PICKLE (PKL) domains in regulating drought tolerance and the protein stability of PKL in *Arabidopsis*. (a, b) Drought stress responses (a) and survival rates (b) of soil-grown Col-0, the *pkl* mutant, *PKLp:PKL-GFP/pkl* (PKL), *PKLp:PKLΔPHD-GFP/pkl* (ΔPHD), *PKLp:PKLΔChromo-GFP/pkl* (ΔChromo), *PKLp:PKLΔATPase-GFP/pkl* (ΔATPase), and *PKLp:PKLΔDBD-GFP/pkl* (ΔDBD) transgenic plants after drought treatment. Four-week-old plants were dehydrated for 7–10 d and then rehydrated for 2 d. Values in (b) represent means ± SD obtained from three replicates with 48 plants per replicate. Different letters represent significant differences based on one-way ANOVA ($P < 0.05$). (c) Water loss rates of leaves detached from Col-0, the *pkl* mutant, PKL, ΔPHD, ΔChromo, ΔATPase, and ΔDBD. Means and SD of water loss rates were obtained from three replicates. Statistical significance was determined by Student's *t*-test: *, $P < 0.05$; **, $P < 0.01$. (d) Reverse transcriptase–polymerase chain reaction (RT-qPCR) analysis showing the transcript levels of *PKL* in 7-d-old seedlings of PKL, ΔPHD, ΔChromo, ΔATPase, and ΔDBD. Values shown are mean ± SD (n = 3). (e) Protein levels of PKL-GFP in 7-d-old PKL, ΔPHD, ΔChromo, ΔATPase, and ΔDBD seedlings. Actin was used as a loading control. (f) Protein levels of PKL-GFP in 7-d-old PKL and ΔDBD seedlings with or without 50 μM MG132 treatment. Actin was used as a loading control. The relative protein levels were quantified using ImageJ. (g) RT-qPCR analysis showing the transcript levels of *PKL* in 7-d-old PKL and ΔDBD seedlings with or without 50 μM MG132 treatment. The relative transcript levels were normalized to *ACTIN7*. Values shown are mean ± SD (n = 3).

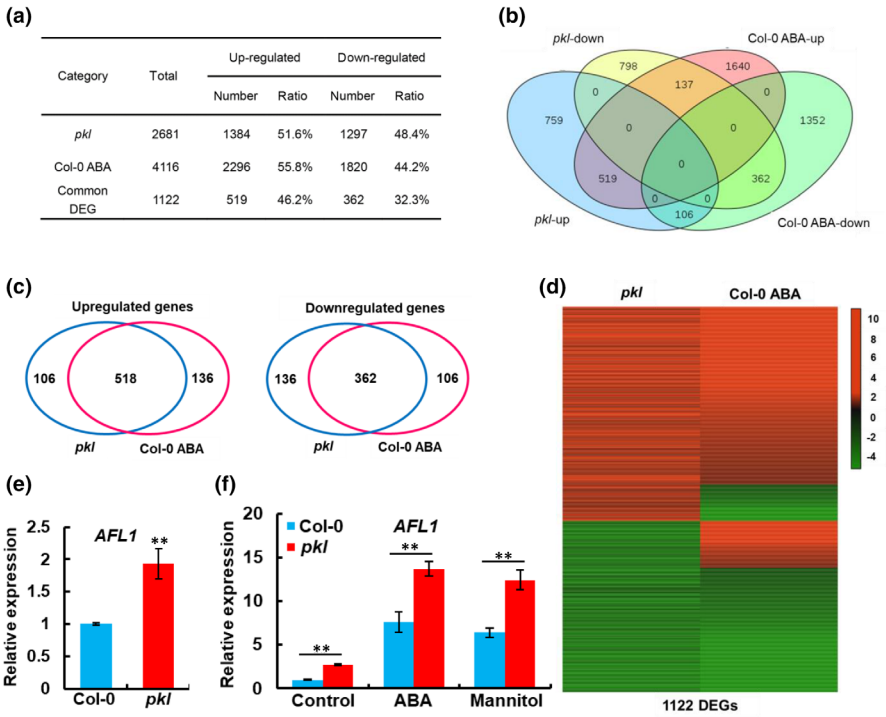

Category	Total	Up-regulated		Down-regulated	
		Number	Ratio	Number	Ratio
pkl	2681	1384	51.6%	1297	48.4%
Col-0 ABA	4116	2296	55.8%	1820	44.2%
Common DEG	1122	519	46.2%	362	32.3%

Fig. 3 PICKLE (PKL)-regulated genes revealed by RNA sequencing (RNA-seq) and reverse transcriptase–polymerase chain reaction (RT-qPCR). (a) Numbers of total, upregulated and downregulated genes in the *pkl* mutant, the abscisic acid (ABA)-treated Col-0 and their common differentially expressed genes (DEGs). (b) Venn diagram showing overlaps between upregulated and downregulated DEGs in the *pkl* mutant and the ABA-treated Col-0. (c) Venn diagram showing numbers of differentially expressed genes in the *pkl* mutant and Col-0 treated with 50 μM ABA. (d) Heat map showing the expression patterns of 1122 common DEGs with the criteria: $\log_2$ fold change ≥ 1 ($P \leq 0.05$) for the upregulated genes and $\log_2$ fold change ≤ −1 ($P \leq 0.05$) for the downregulated genes, respectively. (e) RT-qPCR assays confirming the expression levels of *AFL1* in Col-0 and the *pkl* mutant. (f) RT-qPCR assay showing the expression patterns of *AFL1* in Col-0 and the *pkl* mutant in response to ABA and mannitol treatments. The 10-d-old seedlings were collected at 2 h after ABA or mannitol treatment. The relative expression levels were normalized to *ACTIN7*. Values shown are mean ± SD ($n = 3$). Statistical significance was determined by Student's *t*-test: **, $P < 0.01$.

levels of *PKL* using RT-qPCR assays. The result showed that the expression levels of *PKL* were largely similar in the PKL and ΔDBD transgenic plants with or without MG132 treatment (Fig. 2g). Taken together, these results support the view that the DBD domain is required for the protein stability of PKL.

Transcriptome analysis revealing that PKL represses the expression of drought-tolerant gene *AFL1*

To explore the molecular basis of PKL-regulated drought tolerance, we performed transcriptomic analysis of Col-0 and the *pkl* mutant by RNA sequencing (RNA-seq). DEGs were identified using the criteria: $|\log_2$ fold change$| \geq 1$ ($P \leq 0.05$). We identified 2681 (1384 upregulated and 1297 downregulated) DEGs in the *pkl* mutant (*pkl* vs Col-0, labeled as *pkl*) and 4116 (2296 upregulated and 1820 downregulated) DEGs in the Col-0 with ABA treatment (Col-0 ABA vs Col-0, labeled as Col-0 ABA; Fig. 3a,b; Dataset S1, S2). We then compared the expression profiles of *pkl* with Col-0 ABA and found that 1122 genes were common DEGs in the *pkl* mutant (42.9%) and Col-0 with ABA treatment (27.3%; Fig. 3a,b; Dataset S3). Notably, among these 1122 genes, most of the upregulated genes (83%) in the *pkl* mutant were also upregulated in Col-0 with ABA treatment, and most of the downregulated genes (72.7%) in the *pkl* mutant were also downregulated in Col-0 with ABA treatment (Fig. 3c). The common 1122 DEGs with the criteria '$|\log_2$ fold change$| \geq 1$ ($P \leq 0.05$)' were clustered together in a heat map of expression levels (Fig. 3d; Dataset S3). Gene Ontology (GO) enrichment analyses were performed. The results showed that PKL-regulated genes, ABA-regulated genes, and 1122 common DEGs are all related to abiotic stress responses and hormone responses such as cold, wounding, salt stress, water deprivation, ABA, and jasmonic acid (Figs S5, S6; Dataset S1–S3).

We noted that the common DEGs include drought tolerance-related genes *RD29B*, *COR15A*, *HAI2*, *DREB2B*, and *At14a-like1* (*AFL1*), cold stress-related genes *COR15B*, *DREB1B*, *OLE1*, and *OLE2*, salt stress-related genes *NAC2* and *CIPK16* and some genes involved in plant hormone pathways *ABA3*, *AFP4*, and *JAZ1* (Dataset S3). Among these genes, *COR15A* is generally used as a marker gene for abiotic stress responses and *HAI2*, encoding a protein phosphatase 2Cs (PP2Cs), functions as a negative regulator of drought tolerance (Govinal *et al.*, 2012; Zhang *et al.*, 2013). We tested the expression levels of *COR15A* and *HAI2* using RT-qPCR assays to confirm the RNA-seq data (Fig. S7). Notably, *AFL1* has been demonstrated to be involved in membrane-associated drought

sensing or signaling (Kumar *et al.*, 2015). Consistent with the RNA-seq data, RT-qPCR analysis confirmed that the expression levels of *AFL1* in the *pkl* mutant were higher than those in Col-0 (Fig. 3e). Furthermore, we showed that the expression levels of *AFL1* could also be induced by ABA and mannitol treatments, and the induction was enhanced in the *pkl* mutant (Fig. 3f). Moreover, we also investigated the regulatory effects of different PKL domains on the expression of *AFL1*. RT-qPCR analyses showed that the full-length PKL could suppress the enhanced expression levels of *AFL1* in the *pkl* mutant; whereas the PKLΔPHD, PKLΔChromo, and PKLΔATPase truncated proteins could partially suppress or failed to suppress the increased expression levels of *AFL1* in the *pkl* mutant, suggesting that the chromo domain and ATPase domain as well as the PHD domain are necessary for PKL function in repressing the expression of *AFL1* (Fig. S8).

PKL associates with and facilitate H3K27me3 deposition at the chromatin of *AFL1*

To investigate the molecular relevance of the PKL-*AFL1* interaction, we performed ChIP-qPCR assays using anti-GFP antibody to probe *PKLp:PKL-GFP/pkl* transgenic plants. The result showed that PKL was significantly enriched in the promoter region (P2), 5′UTR (P4) and gene body (P5, P6, and P7) of *AFL1*, indicating that PKL associates with the chromatin regions of *AFL1* (Fig. 4a,b). Previous studies have reported that PKL promotes the deposition of H3K27me3, a histone mark associated with transcriptional repression (Zhang *et al.*, 2012, 2014; Jing *et al.*, 2013; Carter *et al.*, 2018). To investigate whether PKL affects the H3K27me3 deposition at the *AFL1* locus, we performed ChIP-qPCR assays using the Col-0, *pkl* and *PKLp:PKL-GFP/pkl* seedlings with the anti-H3K27me3 antibody. The results showed that H3K27me3 was indeed enriched in the promoter region (P2), 5′UTR (P3 and P4), and gene body (P5, P6, and P7) of *AFL1*, whereas the deposition of H3K27me3 at the chromatin regions of *AFL1* was significantly reduced in the *pkl* mutant, which could be restored in the *PKLp:PKL-GFP/pkl* transgenic plants (Fig. 4c). Taken together, these results indicate that PKL associates with the chromatin regions of *AFL1* to repress its transcription by facilitating PRC2-mediated H3K27me3 deposition.

PKL-mediated regulation of drought tolerance is dependent on *AFL1*

Given PKL directly represses the expression of *AFL1*, we wondered whether *AFL1* is required for PKL-mediated regulation of drought tolerance. To address this question, we generated the gene-edited *afl1* mutant in the Col-0 background using the CRISPR (clustered regularly interspaced short palindromic repeats)/Cas9 (CRISPR-associated nuclease 9) system (Yan *et al.*, 2015; Fig. S9). Furthermore, we introduced the *afl1* mutation into the *pkl* mutant background by genetic crossing. Then, we observed the drought stress responses of Col-0, *pkl*, *afl1*, and the *pkl afl1* double mutant. We stopped irrigation of 4-wk-old plants for 7–10 d and then rewatered them. Plant survival rates were scored 2 d after rewatering. The results showed that the *afl1* mutation could completely suppress the drought-tolerant phenotype of the *pkl* mutant (Fig. 4d–f). We also analyzed stomatal aperture of Col-0, *pkl*, *afl1*, and the *pkl afl1* double mutant in response to mannitol treatment. The result showed that stomatal aperture in the leaves of *pkl* mutant was smaller than that in Col-0 in the presence of 300 mM mannitol treatment, while the stomatal aperture in the leaves of both *afl1* mutant and the *pkl afl1* double mutant was similar to that in Col-0 (Fig. S10). These results demonstrate that the drought-tolerant phenotype of the *pkl* mutant is dependent on *AFL1*. Intriguingly, the growth defect of *pkl* was also suppressed by the *afl1* mutation (Fig. 4d).

MMS21 and PKL physically interact to additively regulate drought tolerance

MMS21 encodes a functional SUMO E3 ligase, which has been reported to regulate the stability of target proteins and also negatively regulate drought tolerance (Zhang *et al.*, 2013, 2017; Yu *et al.*, 2019). Therefore, we wondered whether MMS21 is associated with PKL. LCI assays were first applied to investigate whether PKL physically interacts with MMS21 in *N. benthamiana* leaves. For this assay, we generated nLUC-PKL and cLUC-MMS21 constructs. Only when nLUC-PKL and cLUC-MMS21 were co-expressed in *N. benthamiana* leaves, strong LUC activity could be detected (Fig. 5a), suggesting that PKL could interact with MMS21. Furthermore, we confirmed that PKL physically interacts with MMS21 using BiFC assays. MMS21 was fused to the N-terminal part of YFP (nYFP-MMS21) and PKL was fused to the C-terminal part of YFP (cYFP-PKL). The result showed that the interaction of PKL and MMS21 occurs in the nucleus (Fig. 5b). Finally, we conducted Co-IP assays using the Col-0 and *35S:Myc-MMS21* seedlings to confirm the interaction between PKL and MMS21 *in planta*. The result showed that PKL was immunoprecipitated by Myc-MMS21, demonstrating that PKL interacts with MMS21 *in vivo* (Fig. 5c). Taken together, we conclude that MMS21 interacts with PKL.

To analyze the genetic relationship between MMS21 and PKL in regulating drought tolerance, we generated the *mms21-1 pkl* double mutant by genetic crossing. Then we examined the drought stress responses of Col-0, *mms21-1*, *pkl*, and *mms21-1 pkl* plants. As expected, after drought treatment, the *mms21-1* and *pkl* single mutants grew well compared with Col-0 (Fig. 5d). Significantly, we found that the *mms21-1 pkl* double mutant grew better than those single mutants (Fig. 5d). After rewatering, the survival rates of the *mms21-1* mutant (*c.* 88% on average) and the *pkl* mutant (*c.* 74% on average) were higher than that of Col-0 (*c.* 30% on average); the survival rate of the *mms21-1 pkl* double mutant (*c.* 98% on average) was higher than those of the single mutants (Fig. 5e). We finally conducted water loss assays in detached leaves. As expected, the detached leaves of the *mms21-1* mutant and the *pkl* mutant lost water slower than Col-0 (Fig. 5f). Interestingly, the water loss rate of the *mms21-1 pkl* double mutant was significantly lower than those of single mutants (Fig. 5f). Taken together, these results demonstrate that MMS21 and PKL additively regulate *Arabidopsis* drought tolerance.

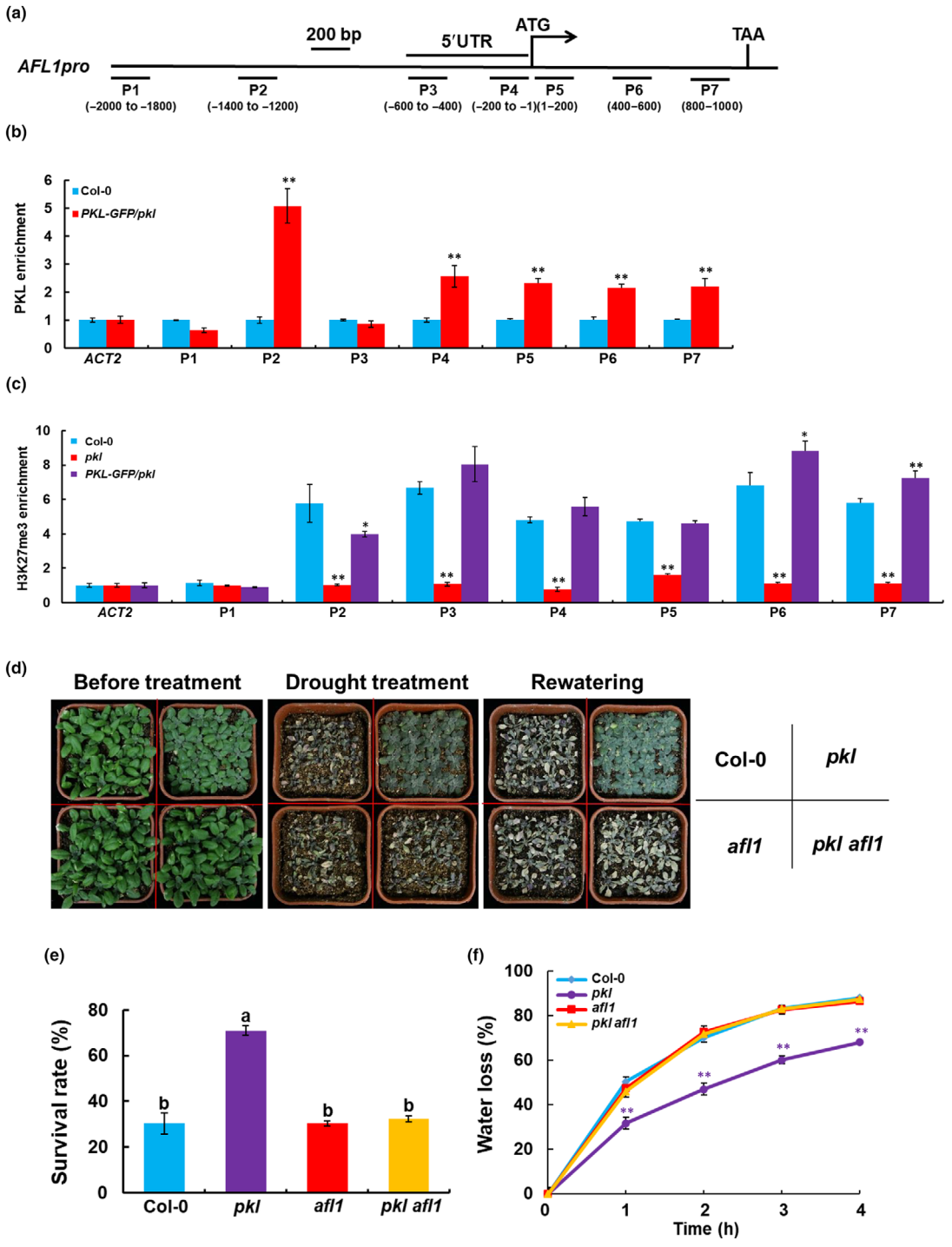

Fig. 4 PICKLE (PKL) associates with and facilitate H3K27me3 deposition at the chromatin of *AFL1* to regulate *Arabidopsis* drought tolerance. (a) Diagram of *AFL1*. P1–P7 indicate the positions of primers for chromatin immunoprecipitation (ChIP)-qPCR analyses. (b) ChIP-qPCR analysis showing the association of PKL with the chromatin regions of *AFL1* using anti-GFP antibody. The 10-d-old Col-0 and *PKLp:PKL-GFP/pkl* seedlings were used for ChIP assays. The enrichments were relative to INPUT. Data were relative to the *ACT2* internal control. Values shown are mean ± SD ($n = 3$). Statistical significance was determined by Student's *t*-test: **, $P < 0.01$. (c) ChIP-qPCR analysis showing the H3K27me3 deposition at the chromatin regions of *AFL1*. The 10-d-old Col-0, the *pkl* mutant, and *PKLp:PKL-GFP/pkl* seedlings were used for ChIP assays. The enrichments were relative to INPUT. Data were relative to the *ACT2* internal control. Values shown are mean ± SD ($n = 3$). Statistical significance was determined by Student's *t*-test: **, $P < 0.01$. (d, e) Drought stress responses (d) and survival rates (e) of soil-grown Col-0, *pkl*, *afl1*, and the *pkl afl1* double mutant. Four-week-old plants were dehydrated for 7–10 d and then rehydrated for 2 d. Values in (e) represent means ± SD obtained from three replicates with 48 plants per replicate. Different letters represent significant differences based on one-way ANOVA ($P < 0.05$). (f) Water loss rates of leaves detached from Col-0, *pkl*, *afl1*, and the *pkl afl1* double mutant. Means and SD of water loss rates were obtained from three replicates. Statistical significance was determined by Student's *t*-test: **, $P < 0.01$.

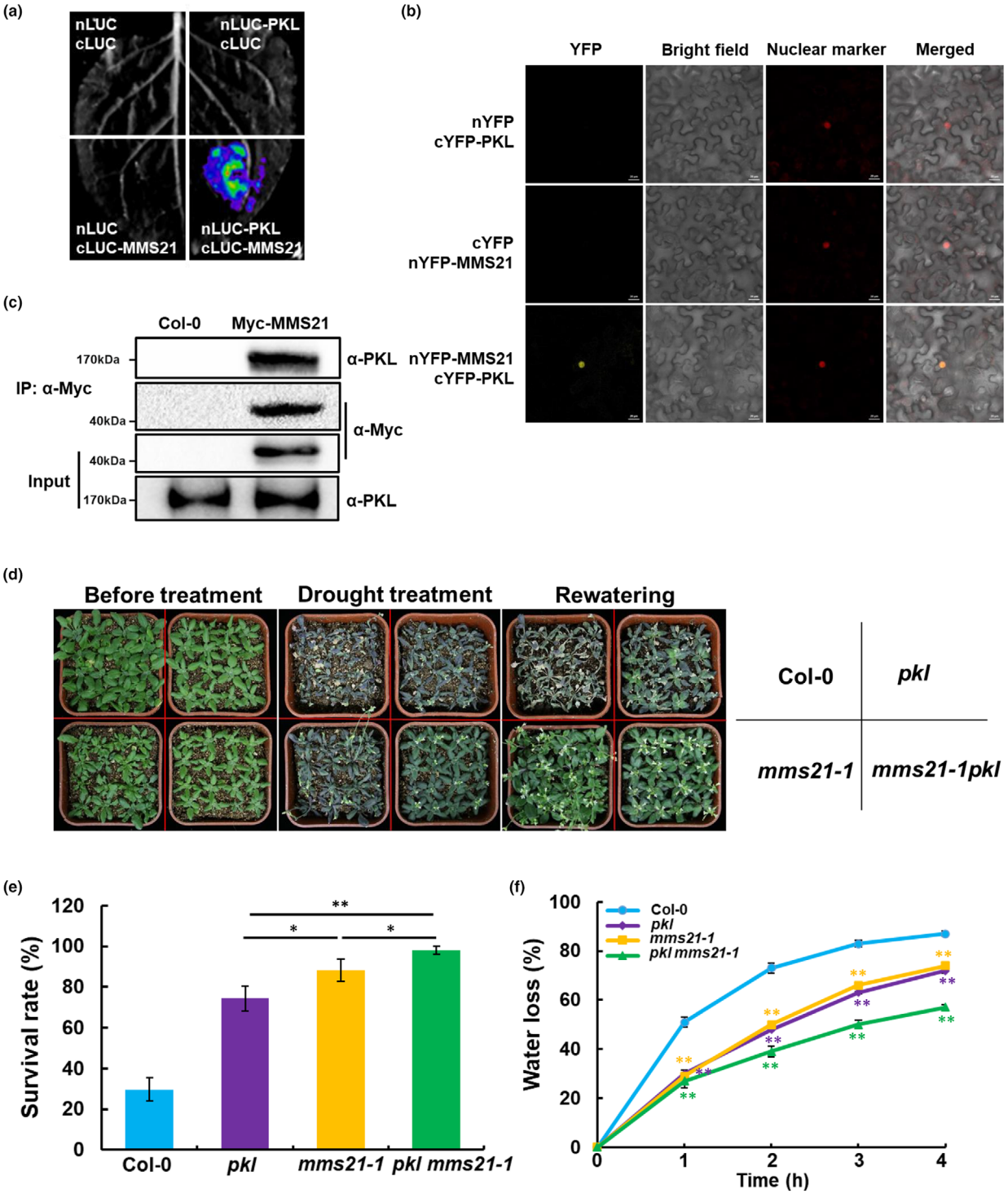

Fig. 5 MMS21 and PICKLE (PKL) physically interact to additively regulate *Arabidopsis* drought tolerance. (a) Luciferase complementation imaging (LCI) assays showing that PKL interacts with MMS21 in *N. benthamiana* leaves. (b) Bimolecular fluorescence complementation (BiFC) assays showing the interaction of PKL and MMS21 in nucleus of *N. benthamiana*. The RFP-AHL22 vector was co-transformed as a nuclear localization marker (red signal). Bars, 20 μm. (c) Co-IP assays showing the interaction between PKL and MMS21 *in vivo*. Total proteins were extracted from 7-d-old seedlings of Col-0 and the *35S:Myc-MMS21* transgenic plants, immunoprecipitated with anti-Myc antibody and analyzed by immunoblotting using anti-PKL antibody. (d, e) Drought stress responses (d) and survival rates (e) of soil-grown Col-0, *pkl*, *mms21-1*, and the *pkl mms21-1* double mutant. Four-week-old plants were dehydrated for 7–10 d and then rehydrated for 2 d. Values in (e) represent means ± SD obtained from three replicates with 48 plants per replicate. Statistical significance was determined by Student's *t*-test: *, $P < 0.05$; **, $P < 0.01$. (f) Water loss rates of leaves detached from Col-0, *pkl*, *mms21-1*, and the *pkl mms21-1* double mutant. Means and SD of water loss rates were obtained from three replicates. Statistical significance was determined by Student's *t*-test: **, $P < 0.01$.

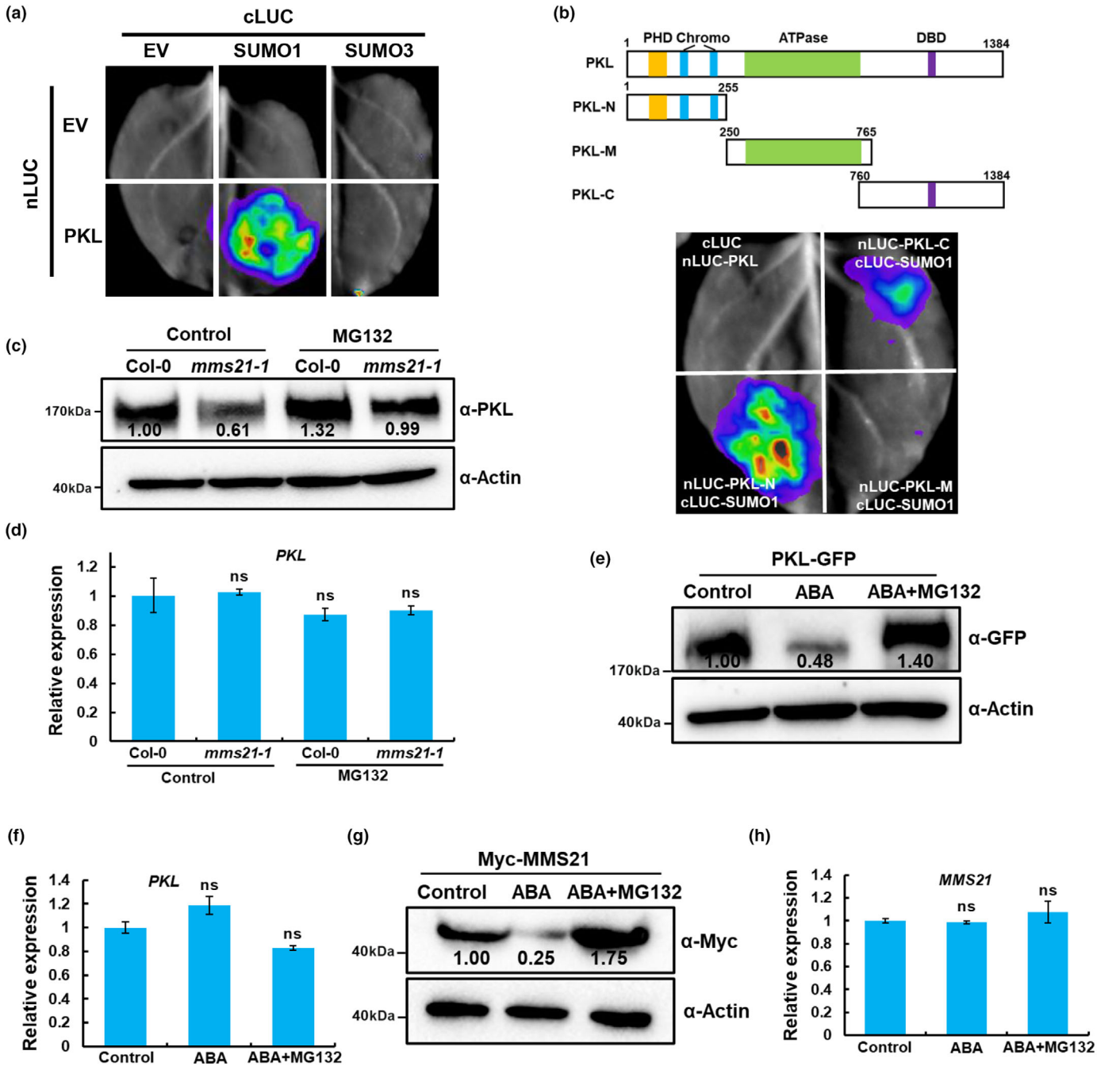

Fig. 6 PICKLE (PKL) is covalently modified by SUMO1 to enhance the protein stability of PKL in *Arabidopsis*. (a) Luciferase complementation imaging (LCI) assays showing that PKL interacts with SUMO1 in *N. benthamiana* leaves. (b) LCI assays showing the physical interaction of SUMO1 with PKL-N and PKL-C in *N. benthamiana* leaves. (c) Immunoblotting assays showing the protein levels of PKL in 10-d-old seedlings of Col-0 and the *mms21-1* mutant with or without MG132 treatment. Actin was used as a loading control. The relative protein levels were quantified using ImageJ. (d) Reverse transcriptase–polymerase chain reaction (RT-qPCR) analysis showing the transcript levels of *PKL* in 10-d-old seedlings of Col-0 and the *mms21-1* mutant with or without MG132 treatment. The relative transcript levels were normalized to *ACTIN7*. Values shown are mean ± SD ($n = 3$). ns, not significant. (e) Immunoblotting assays showing the protein levels of PKL in 10-d-old *PKLp:PKL-GFP* seedlings with or without abscisic acid (ABA) and MG132 treatments. Samples were collected at 2 h after ABA and MG132 treatments. Actin was used as a loading control. The relative protein levels were quantified using ImageJ. (f) RT-qPCR assay showing the transcript levels of *PKL* in 10-d-old *PKLp:PKL-GFP* seedlings with or without ABA and MG132 treatments. The relative transcript levels were normalized to *ACTIN7*. Values shown are mean ± SD ($n = 3$). ns, not significant. (g) Immunoblotting assays showing the protein levels of MMS21 in 10-d-old *35S:Myc-MMS21* seedlings with or without ABA and MG132 treatments. Samples were collected at 2 h after ABA and MG132 treatments. Actin was used as a loading control. The relative protein levels were quantified using ImageJ. (h) RT-qPCR assay showing the transcript levels of *MMS21* in 10-d-old *35S:Myc-MMS21* seedlings with or without ABA and MG132 treatments. The relative transcript levels were normalized to *ACTIN7*. Values shown are mean ± SD ($n = 3$). ns, not significant.

PKL interacts with SUMO1

Because MMS21 interacts with PKL, we speculated that PKL might be a substrate of SUMOylation. Given there are different SUMO homologues in *Arabidopsis*, we detected the physical association of PKL and SUMO molecules using LCI assays. For the assays, SUMO1 and SUMO3 were separately fused to the C-terminal part of LUC to generate the cLUC-SUMO1 and cLUC-SUMO3 constructs. Interestingly, only when cLUC-SUMO1 and nLUC-PKL were co-expressed in *N. benthamiana* leaves, strong LUC activity could be detected (Fig. 6a), suggesting that SUMO1 but not SUMO3 is physically associated with PKL. We further generated the nLUC-PKL-N (including the PHD domain and Chromo domain), nLUC-PKL-M (including the ATPase domain), and nLUC-PKL-C (including the DBD domain) constructs for LCI assays (Fig. 6b). After co-infiltration of *N. benthamiana* leaves, we found that strong LUC activity was detected in the samples co-expressing nLUC-PKL-N and cLUC-SUMO1 and weak LUC activity was detected in the samples co-expressing nLUC-PKL-C and cLUC-SUMO1, whereas no luminescence signal was observed in the samples co-expressing nLUC-PKL-M and cLUC-SUMO1 (Fig. 6b). These results suggest that the N-terminal part of PKL mainly mediates the interaction with SUMO1.

MMS21 promotes the stabilization of PKL

To determine whether the protein stability of PKL is regulated by MMS21, we first analyzed the protein levels of PKL in Col-0 and the *mms21-1* mutant. The immunoblotting assays showed that the protein level of PKL was obviously reduced in the *mms21-1* mutant compared with that in Col-0 (Fig. 6c). We also analyzed the protein level of PKL in Col-0 and the *mms21-1* mutant in response to MG132 treatment. The results showed that the protein level of PKL in the *mms21-1* mutant could be rescued by MG132 treatment (Fig. 6c). RT-qPCR analysis showed that the transcript levels of *PKL* were comparable in Col-0 and the *mms21-1* mutant with or without MG132 treatment (Fig. 6d), indicating that MMS21 may be involved in the regulation of PKL protein stability. To further evaluate the effect of MMS21 on the protein stability of PKL, 10-d-old seedlings of Col-0, and the *mms21-1* mutant were treated with the protein biosynthesis inhibitor cycloheximide (CHX) for 0, 2, 4, and 6 h, and then immunoblotting assays were performed with anti-PKL antibody. The results indicated that the degradation of PKL protein occurred more slowly in Col-0 than that in the *mms21-1* mutant, indicating that MMS21 promotes the stabilization of PKL (Fig. S11). We also found that ABA treatment reduced the protein level of PKL, which could be prevented by MG132 treatment (Fig. 6e). The transcript levels of *PKL* in Col-0 were not affected by ABA and MG132 treatments (Fig. 6f). Furthermore, we wondered whether ABA and MG132 treatments also affect the protein level of MMS21. To test this idea, we investigated the protein level of MMS21 in the *35S:Myc-MMS21* transgenic seedlings with ABA and MG132 treatments. The immunoblotting assays showed that the protein levels of MMS21 were decreased after ABA treatment, whereas this ABA effect was inhibited by the MG132 treatment (Fig. 6g). RT-qPCR analysis showed that the transcript levels of *MMS21* were not affected by ABA and MG132 treatments (Fig. 6h). Taken together, these results suggest that MMS21 promotes the stabilization of PKL.

Discussion

Drought stress causes substantial losses in crop production per year worldwide, threatening global food security. Drought stress has even been thought of as a "cancer" to crop plants, owing to its complexity and destructiveness. Thus, there is an urgent demand for improving crop drought tolerance through biotechnology. Molecular breeding is an effective and sustainable strategy to improve crop drought tolerance. Disruption of the drought-susceptible genes in crops by natural variations or CRISPR/Cas9 is an attractive breeding strategy for conferring drought tolerance. In this study, we uncover a novel function for PKL in the negative regulation of drought tolerance. Loss of PKL function conferred an enhanced drought tolerance phenotype (Fig. 1). Because drought tolerance is a key trait for crop breeding, it will be interesting to investigate the role of PKL homologues in crop drought tolerance and utilize them to improve drought tolerance in key agricultural species.

PKL is a CHD3-type epigenetic regulator that mediates the transcriptional silencing through promoting the deposition of a transcriptional repression mark H3K27me3. The ability of PKL to remodel chromatin and modify histones enables it to regulate the expression of thousands of genes. PKL and polycomb group proteins antagonistically determine cell identity and regulate meristem activity in the *Arabidopsis* root by modulating levels of H3K27me3 (Aichinger *et al.*, 2009, 2011). Moreover, it has been shown that PKL is enriched at genome loci decorated by H3K27me3 (Zhang *et al.*, 2008). A recent study revealed that PKL could interact with the transcription factors VAL1/2 to repress the expression of *ABI3* and *AGL15* in regulating the seed-to-seedling transition (Liang *et al.*, 2022). Our transcriptome analysis revealed that PKL represses the transcription of the drought tolerance-related gene *AFL1* (Fig. 3). Our results demonstrated that PKL associates with the chromatin regions of *AFL1* and represses its transcription via facilitating the H3K27me3 deposition at the chromatin regions of *AFL1* (Fig. 4a–c). Analysis of the genetic relationship between *PKL* and *AFL1* proved that PKL genetically acts upstream of *AFL1* to regulate *Arabidopsis* drought tolerance (Fig. 4d–f).

Interestingly, we noticed that the truncated protein of PKLΔDBD was undetectable in the transgenic plants, indicating that the DBD domain plays an essential role for the protein stability of PKL (Fig. 2f). And the MG132 treatment could restore the protein level of PKLΔDBD, indicating that PKL binding to the chromatin favors its stabilization (Fig. 2f). Simultaneously, we found that ABA treatment led to the degradation of PKL and this ABA effect could be prevented by MG132 treatment (Fig. 6e). However, the E3 ubiquitin ligase that mediates the ubiquitination of PKL still remains unknown. SUMOylation and ubiquitination are two kinds of post-translational modifications,

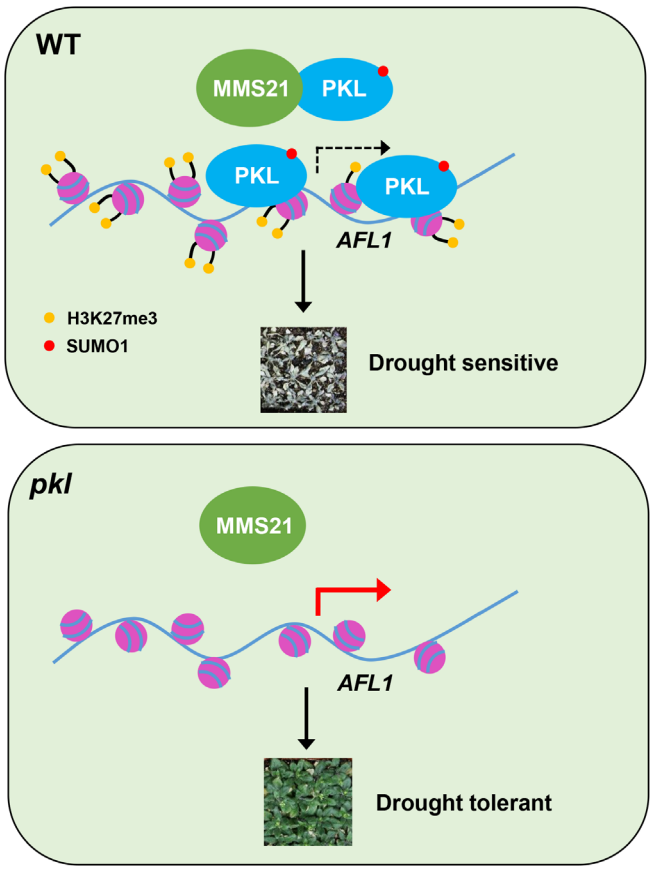

Fig. 7 A proposed working model for the MMS21-PKL-*AFL1* module in regulating *Arabidopsis* drought tolerance. In the WT, MMS21 interacts with and stabilizes the epigenetic regulator PKL, which directly represses the transcription of *AFL1* via H3K27me3 deposition, leading to the drought-sensitive phenotype. In the *pkl* mutant, the activation of *AFL1* transcription confers a drought-tolerant phenotype. Black solid arrows, the resulting effect on plant drought response; black dashed arrow, transcription repression; red solid arrow, transcription activation. PKL, PICKLE.

which antagonistically modulate the protein stability (Geoffroy & Hay, 2009). MMS21 acts as a SUMO E3 ligase that regulates the stability of target proteins (Zhang *et al.*, 2013, 2017; Yu *et al.*, 2019). We demonstrated that MMS21 interacts with and promotes the protein stability of PKL (Figs 5a–c, 6). However, the genetic interaction analysis demonstrated that MMS21 and PKL additively regulate plant drought tolerance (Fig. 5d–f). To explain this genetic result, we speculated that in addition to PKL, MMS21 may also target other proteins in the regulation of plant drought tolerance.

Based on the genetic and biochemical evidence presented in this study, we propose a working model for the MMS21-PKL-*AFL1* module in regulating *Arabidopsis* drought tolerance (Fig. 7). In the wild type (WT), MMS21 interacts with and stabilizes the epigenetic regulator PKL, which directly represses the transcription of *AFL1* via H3K27me3 deposition, leading to the drought-sensitive phenotype. In the *pkl* mutant, the derepression of *AFL1* transcription causes a drought-tolerant phenotype. Unraveling the molecular basis underlying plant responses to drought stress will be necessary for engineering drought stress-resilient crops in the future. And the corresponding homologues of PKL, MMS21 and AFL1 are also contained in the major crop species such as rice, maize, and wheat (Figs S12–S14; Dataset S4–S6). It will be meaningful to investigate the functions of these proteins in staple crops and exploit their utilization to enhance crop drought tolerance in the future.

It has been well known that ABA plays important roles in abiotic stress adaptation, such as drought stress, cold stress, and salt stress (Cutler *et al.*, 2010; Finkelstein, 2013; Chen *et al.*, 2020). ABA also regulates multiple processes of plant growth and development, including seed germination, seedling establishment, root growth, stomatal movement, flowering, and leaf senescence (Cutler *et al.*, 2010; Finkelstein, 2013; Chen *et al.*, 2020). ABI5 encodes a basic leucine zipper (bZIP) transcription factor, transducing ABA signals, that regulates seed germination and early seedling growth in *Arabidopsis* (Finkelstein, 1994; Finkelstein & Lynch, 2000). In this study, we found that PKL physically interacts with ABI5 (Fig. S1). We showed that the ABA-hypersensitive seedling growth inhibition phenotype is dependent on the function of ABI5 (Fig. S3). However, the drought-tolerant phenotype of the *pkl* mutant is independent of the function of ABI5 (Fig. S2). Both PKL and MMS21 are negative regulators of plant drought tolerance, while ABA positively regulates plant drought tolerance. In this study, we revealed that ABA positively regulates plant drought tolerance, at least partially, through promoting the degradation of PKL and MMS21 (Fig. 6e,g).

Acknowledgements

We thank Prof. Ernst Aichinger and Prof. Chengwei Yang for providing genetic materials. This research was supported by the Central Public-interest Scientific Institution Basal Research Fund (S2022ZD02) and the Agricultural Science and Technology Innovation Program of Chinese Academy of Agricultural Sciences (CAAS). No conflict of interest is declared.

Competing interests

None declared.

Author contributions

JS designed the research; YJ performed most of the experiments with the assistance of ZY, RY and YZ; WQ and YZ analyzed the data; YJ and JS wrote the manuscript.

ORCID

Yexing Jing https://orcid.org/0000-0001-9716-4914
Weihua Qiao https://orcid.org/0000-0001-9876-3054
Jiaqiang Sun https://orcid.org/0000-0002-3448-6956
Ruizhen Yang https://orcid.org/0009-0000-7454-7699
Ziyi Yang https://orcid.org/0009-0001-3137-4393
Yunwei Zhang https://orcid.org/0009-0007-4522-7275
Yun Zhou https://orcid.org/0000-0001-6179-5407

Data availability

The data that support the findings of this study are available in the article and its Supporting Information files. The RNA-sequencing data have been deposited in the National Center for Biotechnology Information (NCBI) Sequence Read Archive (SRA): PRJNA917592, https://www.ncbi.nlm.nih.gov/bioproject/PRJNA917592.

References

Aichinger E, Villar CB, Di Mambro R, Sabatini S, Kohler C. 2011. The CHD3 chromatin remodeler PICKLE and polycomb group proteins antagonistically regulate meristem activity in the Arabidopsis root. *Plant Cell* **23**: 1047–1060.

Aichinger E, Villar CBR, Farrona S, Reyes JC, Hennig L, Kohler C. 2009. CHD3 proteins and polycomb group proteins antagonistically determine cell identity in Arabidopsis. *PLoS Genetics* **5**: e1000605.

Carter B, Bishop B, Ho KK, Huang R, Jia W, Zhang H, Pascuzzi PE, Deal RB, Ogas J. 2018. The chromatin remodelers PKL and PIE1 act in an epigenetic pathway that determines H3K27me3 homeostasis in Arabidopsis. *Plant Cell* **30**: 1337–1352.

Chen H, Zou Y, Shang Y, Lin H, Wang Y, Cai R, Tang X, Zhou JM. 2008. Firefly luciferase complementation imaging assay for protein-protein interactions in plants. *Plant Physiology* **146**: 368–376.

Chen K, Li GJ, Bressan RA, Song CP, Zhu JK, Zhao Y. 2020. Abscisic acid dynamics, signaling, and functions in plants. *Journal of Integrative Plant Biology* **62**: 25–54.

Chen Q, Hu T, Li X, Song CP, Zhu JK, Chen L, Zhao Y. 2022. Phosphorylation of SWEET sucrose transporters regulates plant root:shoot ratio under drought. *Nature Plants* **8**: 68–77.

Chen XX, Wang TT, Rehman AU, Wang Y, Qi JS, Li Z, Song CP, Wang BS, Yang SH, Gong ZZ. 2021. Arabidopsis U-box E3 ubiquitin ligase PUB11 negatively regulates drought tolerance by degrading the receptor-like protein kinases LRR1 and KIN7. *Journal of Integrative Plant Biology* **63**: 494–509.

Clough SJ, Bent AF. 1998. Floral dip: a simplified method for *Agrobacterium*-mediated transformation of *Arabidopsis thaliana*. *The Plant Journal* **16**: 735–743.

Cutler SR, Rodriguez PL, Finkelstein RR, Abrams SR. 2010. Abscisic acid: emergence of a core signaling network. *Annual Review of Plant Biology* **61**: 651–679.

Dittrich M, Mueller HM, Bauer H, Peirats-Llobet M, Rodriguez PL, Geilfus CM, Carpentier SC, Al Rasheid KAS, Kollist H, Merilo E *et al.* 2019. The role of Arabidopsis ABA receptors from the PYR/PYL/RCAR family in stomatal acclimation and closure signal integration. *Nature Plants* **5**: 1002–1011.

Finkelstein R. 2013. Abscisic acid synthesis and response. *Arabidopsis Book* **11**: e0166.

Finkelstein RR. 1994. Maternal effects govern variable dominance of two abscisic acid response mutations in *Arabidopsis thaliana*. *Plant Physiology* **105**: 1203–1208.

Finkelstein RR, Lynch TJ. 2000. The Arabidopsis abscisic acid response gene ABI5 encodes a basic leucine zipper transcription factor. *Plant Cell* **12**: 599–609.

Fukaki H, Taniguchi N, Tasaka M. 2006. PICKLE is required for SOLITARY-ROOT/IAA14-mediated repression of ARF7 and ARF19 activity during Arabidopsis lateral root initiation. *The Plant Journal* **48**: 380–389.

Furuta K, Kubo M, Sano K, Demura T, Fukuda H, Liu YG, Shibata D, Kakimoto T. 2011. The CKH2/PKL chromatin remodeling factor negatively regulates cytokinin responses in *Arabidopsis calli*. *Plant Cell Physiology* **52**: 618–628.

Gareau JR, Lima CD. 2010. The SUMO pathway: emerging mechanisms that shape specificity, conjugation and recognition. *Nature Reviews Molecular Cell Biology* **11**: 861–871.

Geoffroy MC, Hay RT. 2009. An additional role for SUMO in ubiquitin-mediated proteolysis. *Nature Reviews Molecular Cell Biology* **10**: 564–568.

Govinal BB, Thao TN, Paul EV. 2012. Unique drought resistance functions of the highly ABA-induced clade A protein phosphatase 2Cs. *Plant Physiology* **160**: 379–395.

Guo AY, Zhu QH, Chen X, Luo JC. 2007. [GSDS: a gene structure display server]. *Yi Chuan* **29**: 1023–1026.

Gupta A, Rico-Medina A, Cano-Delgado AI. 2020. The physiology of plant responses to drought. *Science* **368**: 266–269.

Han D, Lai J, Yang C. 2021. SUMOylation: a critical transcription modulator in plant cells. *Plant Science* **310**: 110987.

He G, Liu J, Dong H, Sun J. 2019. The blue-light receptor CRY1 interacts with BZR1 and BIN2 to modulate the phosphorylation and nuclear function of BZR1 in repressing BR signaling in Arabidopsis. *Molecular Plant* **12**: 689–703.

Hinsch V, Adkins S, Manuela D, Xu ML. 2021. Post-embryonic phase transitions mediated by polycomb repressive complexes in plants. *International Journal of Molecular Sciences* **22**: 7533.

Ho KK, Zhang H, Golden BL, Ogas J. 2013. PICKLE is a CHD subfamily II ATP-dependent chromatin remodeling factor. *Biochimica et Biophysica Acta* **1829**: 199–210.

Hu H, Xiong L. 2014. Genetic engineering and breeding of drought-resistant crops. *Annual Review of Plant Biology* **65**: 715–741.

Hu T, Manuela D, Hinsch V, Xu M. 2022. PICKLE associates with histone deacetylase 9 to mediate vegetative phase change in Arabidopsis. *New Phytologist* **235**: 1070–1081.

Huang L, Yang S, Zhang S, Liu M, Lai J, Qi Y, Shi S, Wang J, Wang Y, Xie Q *et al.* 2009. The Arabidopsis SUMO E3 ligase AtMMS21, a homologue of NSE2/MMS21, regulates cell proliferation in the root. *The Plant Journal* **60**: 666–678.

Ishida T, Fujiwara S, Miura K, Stacey N, Yoshimura M, Schneider K, Adachi S, Minamisawa K, Umeda M, Sugimoto K. 2009. SUMO E3 ligase HIGH PLOIDY2 regulates endocycle onset and meristem maintenance in Arabidopsis. *Plant Cell* **21**: 2284–2297.

Jing Y, Guo Q, Lin R. 2019a. The chromatin-remodeling factor PICKLE antagonizes polycomb repression of FT to promote flowering. *Plant Physiology* **181**: 656–668.

Jing Y, Guo Q, Zha P, Lin R. 2019b. The chromatin-remodelling factor PICKLE interacts with CONSTANS to promote flowering in Arabidopsis. *Plant, Cell & Environment* **42**: 2495–2507.

Jing Y, Zhang D, Wang X, Tang W, Wang W, Huai J, Xu G, Chen D, Li Y, Lin R. 2013. Arabidopsis chromatin remodeling factor PICKLE interacts with transcription factor HY5 to regulate hypocotyl cell elongation. *Plant Cell* **25**: 242–256.

Ju L, Jing YX, Shi PT, Liu J, Chen JS, Yan JJ, Chu JF, Chen KM, Sun JQ. 2019. JAZ proteins modulate seed germination through interaction with ABI5 in bread wheat and Arabidopsis. *New Phytologist* **223**: 246–260.

Kalladan R, Lasky JR, Chang TZ, Sharma S, Juenger TE, Verslues PE. 2017. Natural variation identifies genes affecting drought-induced abscisic acid accumulation in *Arabidopsis thaliana*. *Proceedings of the National Academy of Sciences, USA* **114**: 11536–11541.

Kim H, Hwang H, Hong JW, Lee YN, Ahn IP, Yoon IS, Yoo SD, Lee S, Lee SC, Kim BG. 2012. A rice orthologue of the ABA receptor, OsPYL/RCAR5, is a positive regulator of the ABA signal transduction pathway in seed germination and early seedling growth. *Journal of Experimental Botany* **63**: 1013–1024.

Kim H, Lee K, Hwang H, Bhatnagar N, Kim DY, Yoon IS, Byun MO, Kim ST, Jung KH, Kim BG. 2014. Overexpression of PYL5 in rice enhances drought tolerance, inhibits growth, and modulates gene expression. *Journal of Experimental Botany* **65**: 453–464.

Kumar MN, Hsieh YF, Verslues PE. 2015. At14a-Like1 participates in membrane-associated mechanisms promoting growth during drought in *Arabidopsis thaliana*. *Proceedings of the National Academy of Sciences, USA* **112**: 10545–10550.

Kumar S, Stecher G, Li M, Knyaz C, Tamura K. 2018. MEGA X: molecular evolutionary genetics analysis across computing platforms. *Molecular Biology and Evolution* **35**: 1547–1549.

Kurepa J, Walker JM, Smalle J, Gosink MM, Davis SJ, Durham TL, Sung DY, Vierstra RD. 2003. The small ubiquitin-like modifier (SUMO) protein modification system in *Arabidopsis*. Accumulation of SUMO1 and -2

conjugates is increased by stress. *Journal of Biological Chemistry* **278**: 6862–6872.

Kuromori T, Seo M, Shinozaki K. 2018. ABA transport and plant water stress responses. *Trends in Plant Science* **23**: 513–522.

Lesk C, Rowhani P, Ramankutty N. 2016. Influence of extreme weather disasters on global crop production. *Nature* **529**: 84–87.

Liang Z, Yuan L, Xiong X, Hao Y, Song X, Zhu T, Yu Y, Fu W, Lei Y, Xu J *et al.* 2022. The transcriptional repressors VAL1 and VAL2 mediate genome-wide recruitment of the CHD3 chromatin remodeler PICKLE in Arabidopsis. *Plant Cell* **34**: 3915–3935.

Lim C, Kang K, Shim Y, Yoo SC, Paek NC. 2022. Inactivating transcription factor OsWRKY5 enhances drought tolerance through abscisic acid signaling pathways. *Plant Physiology* **188**: 1900–1916.

Liu M, Shi SF, Zhang SC, Xu PL, Lai JB, Liu YY, Yuan DK, Wang YQ, Du JJ, Yang CW. 2014. SUMO E3 ligase AtMMS21 is required for normal meiosis and gametophyte development in Arabidopsis. *BMC Plant Biology* **14**: 1471–2229.

Liu Y, Lai J, Yu M, Wang F, Zhang J, Jiang J, Hu H, Wu Q, Lu G, Xu P *et al.* 2016. The Arabidopsis SUMO E3 ligase AtMMS21 dissociates the E2Fa/DPa complex in cell cycle regulation. *Plant Cell* **28**: 2225–2237.

Mao H, Jian C, Cheng X, Chen B, Mei F, Li F, Zhang Y, Li S, Du L, Li T *et al.* 2022. The wheat ABA receptor gene TaPYL1-1B contributes to drought tolerance and grain yield by increasing water-use efficiency. *Plant Biotechnology Journal* **20**: 846–861.

Mega R, Abe F, Kim JS, Tsuboi Y, Tanaka K, Kobayashi H, Sakata Y, Hanada K, Tsujimoto H, Kikuchi J *et al.* 2019. Tuning water-use efficiency and drought tolerance in wheat using abscisic acid receptors. *Nature Plants* **5**: 153–159.

Miao J, Li X, Li X, Tan W, You A, Wu S, Tao Y, Chen C, Wang J, Zhang D *et al.* 2020. OsPP2C09, a negative regulatory factor in abscisic acid signalling, plays an essential role in balancing plant growth and drought tolerance in rice. *New Phytologist* **227**: 1417–1433.

Miller MJ, Barrett-Wilt GA, Hua Z, Vierstra RD. 2010. Proteomic analyses identify a diverse array of nuclear processes affected by small ubiquitin-like modifier conjugation in Arabidopsis. *Proceedings of the National Academy of Sciences, USA* **107**: 16512–16517.

Miura K, Jin JB, Hasegawa PM. 2007. Sumoylation, a post-translational regulatory process in plants. *Current Opinion in Plant Biology* **10**: 495–502.

Nambara E, Suzuki M, Abrams S, McCarty DR, Kamiya Y, McCourt P. 2002. A screen for genes that function in abscisic acid signaling in *Arabidopsis thaliana*. *Genetics* **161**: 1247–1255.

Ogas J, Kaufmann S, Henderson J, Somerville C. 1999. PICKLE is a CHD3 chromatin-remodeling factor that regulates the transition from embryonic to vegetative development in Arabidopsis. *Proceedings of the National Academy of Sciences, USA* **96**: 13839–13844.

Okamoto M, Peterson FC, Defries A, Park SY, Endo A, Nambara E, Volkman BF, Cutler SR. 2013. Activation of dimeric ABA receptors elicits guard cell closure, ABA-regulated gene expression, and drought tolerance. *Proceedings of the National Academy of Sciences, USA* **110**: 12132–12137.

Park SY, Peterson FC, Mosquna A, Yao J, Volkman BF, Cutler SR. 2015. Agrochemical control of plant water use using engineered abscisic acid receptors. *Nature* **520**: 545–548.

Perruc E, Kinoshita N, Lopez-Molina L. 2007. The role of chromatin-remodeling factor PKL in balancing osmotic stress responses during Arabidopsis seed germination. *The Plant Journal* **52**: 927–936.

Sadanandom A, Bailey M, Ewan R, Lee J, Nelis S. 2012. The ubiquitin-proteasome system: central modifier of plant signalling. *New Phytologist* **196**: 13–28.

Santosh Kumar VV, Yadav SK, Verma RK, Shrivastava S, Ghimire O, Pushkar S, Rao MV, Senthil Kumar T, Chinnusamy V. 2021. The abscisic acid receptor OsPYL6 confers drought tolerance to indica rice through dehydration avoidance and tolerance mechanisms. *Journal of Experimental Botany* **72**: 1411–1431.

Tian X, Wang Z, Li X, Lv T, Liu H, Wang L, Niu H, Bu Q. 2015. Characterization and functional analysis of pyrabactin resistance-like abscisic acid receptor family in rice. *Rice* **8**: 28.

Tong JK, Hassig CA, Schnitzler GR, Kingston RE, Schreibe SL. 1998. Chromatin deacetylation by an ATP-dependent nucleosome remodelling complex. *Nature* **395**: 917–921.

Vaidya AS, Helander JDM, Peterson FC, Elzinga D, Dejonghe W, Kaundal A, Park SY, Xing Z, Mega R, Takeuchi J *et al.* 2019. Dynamic control of plant water use using designed ABA receptor agonists. *Science* **366**: eaaw8848.

Wang P, Zhao Y, Li Z, Hsu CC, Liu X, Fu L, Hou YJ, Du Y, Xie S, Zhang C *et al.* 2018. Reciprocal regulation of the TOR kinase and ABA receptor balances plant growth and stress response. *Molecular Cell* **69**: 100–112.

Xu M, Hu T, Smith MR, Poethig RS. 2016. Epigenetic regulation of vegetative phase change in Arabidopsis. *Plant Cell* **28**: 28–41.

Xu P, Yang C. 2013. Emerging role of SUMOylation in plant development. *Plant Signaling & Behavior* **8**: e24727.

Yan L, Wei S, Wu Y, Hu R, Li H, Yang W, Xie Q. 2015. High-efficiency genome editing in Arabidopsis using YAO promoter-driven CRISPR/Cas9 system. *Molecular Plant* **8**: 1820–1823.

Yang R, Hong Y, Ren Z, Tang K, Zhang H, Zhu JK, Zhao C. 2019. A role for PICKLE in the regulation of cold and salt stress tolerance in Arabidopsis. *Frontiers in Plant Science* **10**: 900.

Yang Z, Yan B, Dong H, He G, Zhou Y, Sun J. 2021. BIC1 acts as a transcriptional coactivator to promote brassinosteroid signaling and plant growth. *EMBO Journal* **40**: e104615.

Yu M, Meng B, Wang F, He Z, Hu R, Du J, Lai J, Yang C. 2019. A SUMO ligase AtMMS21 regulates activity of the 26S proteasome in root development. *Plant Science* **280**: 314–320.

Yuan D, Lai J, Xu P, Zhang S, Zhang J, Li C, Wang Y, Du J, Liu Y, Yang C. 2014. AtMMS21 regulates DNA damage response and homologous recombination repair in Arabidopsis. *DNA Repair* **21**: 140–147.

Zeevaart JA. 1980. Changes in the levels of abscisic acid and its metabolites in excised leaf blades of xanthium strumarium during and after water stress. *Plant Physiology* **66**: 672–678.

Zha P, Jing Y, Xu G, Lin R. 2017. PICKLE chromatin-remodeling factor controls thermosensory hypocotyl growth of *Arabidopsis*. *Plant, Cell & Environment* **40**: 2426–2436.

Zha P, Liu S, Li Y, Ma T, Yang L, Jing Y, Lin R. 2020. The evening complex and the chromatin-remodeling factor PICKLE coordinately control seed dormancy by directly repressing DOG1 in Arabidopsis. *Plant Communications* **1**: 100011.

Zhang D, Jing Y, Jiang Z, Lin R. 2014. The chromatin-remodeling factor PICKLE integrates brassinosteroid and gibberellin signaling during skotomorphogenic growth in Arabidopsis. *Plant Cell* **26**: 2472–2485.

Zhang H, Bishop B, Ringenberg W, Muir WM, Ogas J. 2012. The CHD3 remodeler PICKLE associates with genes enriched for trimethylation of histone H3 lysine 27. *Plant Physiology* **159**: 418–432.

Zhang H, Rider SD Jr, Henderson JT, Fountain M, Chuang K, Kandachar V, Simons A, Edenberg HJ, Romero-Severson J, Muir WM *et al.* 2008. The CHD3 remodeler PICKLE promotes trimethylation of histone H3 lysine 27. *Journal of Biological Chemistry* **283**: 22637–22648.

Zhang J, Lai J, Wang F, Yang S, He Z, Jiang J, Li Q, Wu Q, Liu Y, Yu M *et al.* 2017. A SUMO ligase AtMMS21 regulates the stability of the chromatin remodeler BRAHMA in root development. *Plant Physiology* **173**: 1574–1582.

Zhang S, Qi Y, Liu M, Yang C. 2013. SUMO E3 ligase AtMMS21 regulates drought tolerance in *Arabidopsis thaliana*. *Journal of Integrative Plant Biology* **55**: 83–95.

Zhu JK. 2002. Salt and drought stress signal transduction in plants. *Annual Review of Plant Biology* **53**: 247–273.

Supporting Information

Additional Supporting Information may be found online in the Supporting Information section at the end of the article.

Dataset S1 Differentially expressed genes in *pkl* vs Col-0.

Dataset S2 Differentially expressed genes in Col-0 abscisic acid vs Col-0.

Dataset S3 Differentially expressed genes in *pkl* vs Col-0 and Col-0 abscisic acid vs Col-0.

Dataset S4 Text file of the protein/gene sequences used for the phylogenetic analysis in Fig. S12.

Dataset S5 Text file of the protein/gene sequences used for the phylogenetic analysis in Fig. S13.

Dataset S6 Text file of the protein/gene sequences used for the phylogenetic analysis in Fig. S14.

Fig. S1 PICKLE physically interacts with ABI5 in *Arabidopsis*.

Fig. S2 PICKLE regulates *Arabidopsis* drought tolerance independently of ABI5.

Fig. S3 PICKLE regulates *Arabidopsis* seedling growth partially dependent on ABI5.

Fig. S4 Plant height of indicated *Arabidopsis* plants.

Fig. S5 Gene Ontology analyses for the differentially expressed genes in the *pkl* mutant and abscisic acid-treated Col-0 seedlings, respectively.

Fig. S6 Gene Ontology analysis for the 1122 common differentially expressed genes.

Fig. S7 RT-qPCR assays confirming the transcriptome data.

Fig. S8 RT-qPCR assays showing the roles of different PICKLE domains in regulating the *AFL1* transcription in *Arabidopsis*.

Fig. S9 Sequences alignment of Col-0 and the *afl1* mutant amplicons.

Fig. S10 *PKL* and *AFL1* genetically interact to regulate stomatal aperture in *Arabidopsis*.

Fig. S11 MMS21 promotes the stabilization of PICKLE in *Arabidopsis*.

Fig. S12 Phylogenetic tree of *PKL* homologues in different plant species.

Fig. S13 Phylogenetic tree of *AFL1* homologues in different plant species.

Fig. S14 Phylogenetic tree of *MMS21* homologues in different plant species.

Table S1 Primers used in this study.

Please note: Wiley is not responsible for the content or functionality of any Supporting Information supplied by the authors. Any queries (other than missing material) should be directed to the *New Phytologist* Central Office.